MDPI

Article

Matrix Non-Structural Model and Its Application in Heat Exchanger Network without Stream Split

Dinghao Li [1], **Jingde Wang** [1], **Wei Sun** [1,*] and **Nan Zhang** [2,*]

1 College of Chemical Engineering, Beijing University of Chemical Technology, Beijing 100029, China
2 Department of Chemical Engineering, The University of Manchester, Manchester M13 9PL, UK
* Correspondence: sunwei@mail.buct.edu.cn (W.S.); nan.zhang@manchester.ac.uk (N.Z.)

Abstract: Heat integration by a heat exchanger network (HEN) is an important topic in chemical process system synthesis. From the perspective of optimization, the simultaneous synthesis of HEN belongs to a mixed-integer and nonlinear programming problem. Both the stage-wise superstructure (SWS) model and the chessboard model are the most widely adopted and belong to structural models, in which a framework is assumed for stream matching, and the global optimal solution outside its feasible domain may be defined by the framework. A node-wise non-structural model (NW-NSM) is proposed to find more universal stream matching options, but it requires a mass of structural variables and extra multiple correction strategies. The aim of this paper is to develop a novel matrix non-structural model (M-NSM) for HEN without stream splits from the perspectives of global optimization methods and superstructure models. In the proposed M-NSM, the heat exchanger position order is quantized by matrix elements at each stream, and a HEN structure is initialized by the random generation of matrix elements. An approach for solving HEN problems based on a matrix real-coded genetic algorithm is employed in this model. The results show that M-NSM provides more flexibility to expand the search region for feasible solutions with higher efficiency than previous models.

Keywords: heat exchanger network synthesis; non-structural model; optimization; matrix real-coded; genetic algorithm

1. Introduction

Chemical production has played an important role in human life and economic development since the first industrial revolution. Production can vary in scale, product categories, raw materials, and even operation modes, but it is always implemented by a series of operation units with certain topology. The heat exchanger network (HEN) is commonly required in most industrial processes, as the temperature of streams to either the reactor or separation unit needs to be specified. According to the process design, some streams need to be heated while others need to be cooled. The HEN can find matches among them to reduce the energy demand from outside utilities, and to effectively control the energy consumption and improve the energy utilization rate of the process system [1]. With increasing energy prices and environmental concerns, the improvement of the HEN has recently attracted more attention.

A modern chemical production facility can produce hundreds of units, or even more, resulting in many opportunities for stream matching, corresponding to different energy-saving and network investments. From the systematic point of view, the motivation for the ideal design of the HEN is to pursue the maximum energy savings with a minimum network investment while this is not feasible in engineering theory, which means there is inherently a tradeoff in utility, the number of heat exchange units, and the heat exchange area. The synthesis of the HEN can be considered as a classical multi-objective optimization problem with constraints [2]. Due to the conflict among objectives and the scale of the

problem, sequential synthesis and simultaneous synthesis have been proposed and applied in both industry and academia.

The sequential approaches are designed to decrease the computing complexity of the issue by breaking it down into three subproblems, which are then tackled consecutively. The pinch design is the most well-known sequential HEN synthesis strategy [3]. In the 1970s, pinch point technology, with fast computation and an explicit physical explanation, was proposed and widely applied, from which the HEN is analyzed and designed based on thermodynamic theory and engineering feasibility, with the aim of recovering heat to the maximum extent and reducing the use of utilities [4]. Pinch analysis employs composite curves, grand composite curves, and grid diagrams to design HENs. Kemp continued his discussion on pinch analysis, focusing on energy targeting, network design, and evolution [5]. Pinch analysis has been widely applied in the industry, and it has shown a significant benefit since its proposal; however, the design of the HEN needs to be finalized by repeatedly adjusting the minimum temperature difference among two matched streams, ΔT_{min}, as well as the method of stream matching within the system, as the choice of ΔT_{min} not only affects the final utility cost but also the network topology. This limitation of the pinch analysis-based methods motivated investigations for more efficient mathematical techniques. With the application of optimization theory, mathematical programming was introduced to the HEN study [6]. Linear programming (LP) for the minimization of utility consumption was established in a transportation model [7]. On this premise, a mixed-integer linear programming (MILP) model is used to solve a MILP problem to identify the smallest number of heat exchangers [8]. Floudas and Grossmann [9–11] proved that the automatic optimization of the HEN could be realized if the superstructure representation method containing all possible network structures was established; thus, the nonlinear programming NLP model was established. Sequential synthesis optimizes the HEN by means of sub-problem decomposition, and it is difficult to weigh the mutual restriction among the utility, number of units, and area. Therefore, the global optimal structure is hard to obtain.

The simultaneous methods addressing all sub-problems are frequently used to identify the overall optimal solution. Instead of relying on thermodynamic objectives and pinch points, this solution focuses on the general HEN economics. Although it produces intricate numerical mathematical models, it also enables us to generate superior integrated solutions using real-world economic measures [12]. The development of simultaneous methods is inseparable from the establishment and development of superstructure models. So far, scholars have developed a variety of superstructure models for synchronous optimization of heat exchange networks. The most popular one is a stage-wised superstructure (SWS) model proposed by Yee and Grossmann [13]. Due to the possible match between hot and cold streams at each stage, this simultaneous synthesis model is widely recognized. In recent years, the chessboard model [14], by which optimization was conducted through network structure sequence modification, has also received more attention. However, both the SWS and the chessboard model are structural models, in which a framework is assumed for stream matching, and the global optimal solution may be outside their feasible domains defined by the framework. To improve the performance of the structural model, a novel node-wise non-structural model (NW-NSM) was first proposed by Xiao Yuan et al. [1], where the heat exchanger location was quantized by nodes at each stream and a HEN structure was formed by the random match between hot and cold nodes. The results showed that the presented NW-NSM possesses more flexibility and freedom to expand the search region for feasible solutions; however, it requires a significant number of structural variables for structure representation and extra multiple strategies for structure validation, so it has a high degree of complexity. Like sequential synthesis approaches, simultaneous synthesis methods enable the acquisition of more exact global optimum costs. As a result, it is still crucial to build simultaneous synthesis models and the robust algorithms that support them in order to minimize computing effort and find the best global solution [15].

From the perspective of optimization, the simultaneous synthesis of the HEN belongs to a mixed-integer and nonlinear programming problem. Based on the optimization techniques employed, they can be divided into two subgroups: those using deterministic techniques, such as linear programming (LP) and nonlinear programming (NLP), and those using stochastic techniques, such as simulated annealing (SA), genetic algorithms (GA), particle swarm optimization (PSO), tabu search (TS), differential evolution (DE), and ant colony optimization (AC). The deterministic methods frequently provide local optimal results [16]. The increased size of the problem has an exponentially decreasing effect on the computational efficiency [17]. Stochastic methods can produce satisfying results in a reasonable computing time since they are flexible, effective, and independent of the initial issues of deterministic methods [18].

Considering the difficulties and deficiencies in the optimization of the existing HEN models, in this paper a novel matrix non-structural model (M-NSM) for HENs without stream splits is proposed to balance the solution accuracy and computational efficiency. The heat exchanger position is described by a matrix element positioned by matching streams, and the matching sequence can be recognized by the element's value if a stream is required to exchange heat with more than one other stream. The M-NSM is easy to expand and visualize. No stage decomposition is required in finding the solution. Moreover, the M-NSM model not only contains part of the heat exchange network structure that cannot be expressed in the current structured model, but it also contains the heat exchange network structure information of the multi-stage structured model.

The rest of the paper is structured as follows: The representation of the M-NSM and the corresponding mathematical description are presented in Section 2. Section 3 provides a detailed introduction to the two-layer optimization algorithm. The M-NSM is applied to three widely studied medium- to large-scale case studies from the literature in Section 4 to verify the M-NSM, and conclusions are summarized in Section 5.

2. Problem Definition and Mathematical Description

In the structured model of the HEN, the fixed structural pattern is assumed for each stage, pre-divided substructure, and the so-called multi-stage network framework. The optimal solution is then obtained by searching all feasible heat exchange matchings and is only generated by a fixed structural pattern, thus making it impossible to evaluate the solution beyond this scope. According to the literature, a better solution could be found outside of the considered substructures. In this sense, a pre-divided substructure limits the free generation of new heat exchange matching in the process of algorithm evolution. Therefore, a novel matrix non-structural model (M-NSM) is proposed based on the perspectives of global optimization methods and non-structural models.

2.1. Matrix Non-Structural Model

The matrix non-structural model (M-NSM) is used to characterize the HEN structure through matrix expression. In the proposed M-NSM, the heat exchanger position is described by a matrix element positioned by matching streams, and the matching sequence can be recognized by the element's value if a stream is required to exchange heat with more than one other stream. In the M-NSM model, a HEN structure is initialized by the random generation of matrix elements. The heat recovery of heat exchangers associated with a stream is subjected to process requirements. Only one hot/cold utility type is permitted in the network, and if the outlet temperature of a stream cannot reach the objective after heat recovery, utilities are used at the stream end as additional energy. Since the current optimization of the HEN with stream splits ignores the cost of the extra pipeline and its required accessories, the results are usually less than their actual network investment [1]. For the practical project, the reduction of the number of stream splits can simplify the network layout. Therefore, the assumption of no stream splits is proposed in the M-NSM, which can effectively reduce the computational complexity of the model. The M-matrix representation of the M-NSM is shown in Figure 1. The M-matrix can be divided into

four submatrices: submatrix A (heat recovery matrix), submatrix B (hot utility matrix), submatrix C (cold utility matrix), and submatrix D (zero matrix).

$$
M = \begin{bmatrix} A & B \\ C & D \end{bmatrix} = \begin{array}{c} \\ C1 \\ C2 \\ \vdots \\ CN \\ \text{Cold utility} \end{array}
\begin{array}{cccccc}
\overset{H1}{} & \overset{H2}{} & \overset{\cdots}{} & \overset{HM}{} & \overset{\text{Hot utility}}{} \\
\begin{bmatrix} a_{11} & a_{12} & \cdots & a_{1M} & b_1 \\ a_{21} & a_{22} & \cdots & a_{2M} & b_2 \\ \vdots & \vdots & \ddots & \vdots & \vdots \\ a_{N1} & a_{N2} & \cdots & a_{NM} & b_N \\ c_1 & c_2 & \cdots & c_M & 0 \end{bmatrix}
\end{array}
$$

Figure 1. M-matrix representation of the M-NSM.

It is important to note that the M-NSM with one stage can incorporate information about the network structure of the SWS and the chessboard model with several stages, and its uncomplicated and unambiguous structure will increase the effectiveness of HEN analysis and optimization. The M-NSM without stage dividing in Figure 2 can express the network structure information of the SWS model with four stages. Furthermore, the M-NSM also includes structures that cannot be expressed in current structural models; for example, the M-matrix structure in Equation (1) cannot be expressed by the basic checkerboard model.

$$
M = \begin{bmatrix}
8 & 7 & 6 & 0 & 5 & 0 & 1 \\
0 & 10 & 9 & 0 & 11 & 0 & 0 \\
0 & 13 & 0 & 0 & 0 & 12 & 1 \\
4 & 3 & 2 & 0 & 0 & 1 & 0 \\
1 & 1 & 1 & 1 & 0 & 0 & 0
\end{bmatrix}
\tag{1}
$$
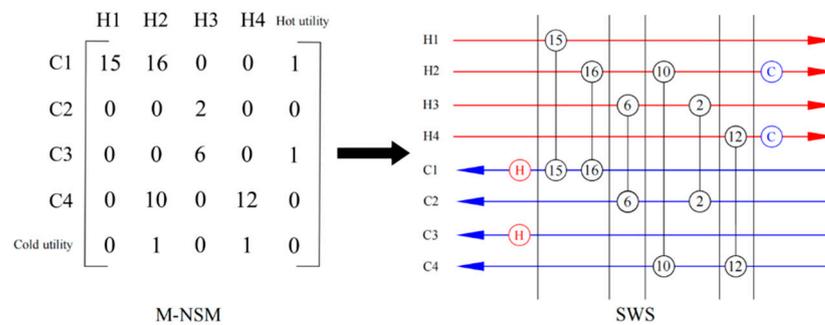
Figure 2. M-NSM used to express the four-stage SWS model structure.

2.1.1. Submatrix A (Heat Recovery Matrix)

Submatrix A represents the matching situation between the hot and cold streams, in which the column represents the hot stream, the row represents the cold stream, and the matrix element a_{ij} represents whether there is a heat exchanger for energy recovery at the location as well as the matching order of stream heat exchange. In order to show the existence of each possible heat exchanger in submatrix A, a multivariable is established. Continuous variables for heat recovery may then be computed using this multivariable. In submatrix A, the multivariate matrix element a_{ij} is an integer in the range of $[0, M \times N]$, where M is the number of hot streams and N is the number of cold streams. As shown in Equation (2), it is a non-negative number. When a_{ij} is 0, there is no heat recovery heat exchanger at this position; when a_{ij} is a positive integer, there is a heat recovery heat exchanger, and the value of a_{ij} represents the matching order among streams.

The larger a_{ij} is, the higher the priority given to matching the corresponding hot and cold streams.

$$\begin{cases} a_{ij} = 0 & (No\ heat\ exchanger) \\ a_{ij} = n\ n \in [1, M \times N] & (Heat\ exchanger\ exists) \end{cases} \tag{2}$$

Considering a HEN with two cold and two hot streams as an example to illustrate the submatrix A = $\begin{bmatrix} a_{11} & a_{12} \\ a_{21} & a_{22} \end{bmatrix}$, the graphical structure expression is shown in Figure 3, where the red dots represent the locations of possible streams matching, with different paths showing that the matching priorities of the streams change. The yellow lines represent the basic paths of the streams, and the blue lines represent the possible optimal flow paths of the streams. As shown in Figure 4, submatrix A can be considered, as a HEN configuration consists of heat exchangers among cold and hot streams only. In Figure 4, there are two feasible matches for the HEN: In Figure 4a, E4 is first assigned followed by E1, while in Figure 4b, the sequence is E4, E3, E2, E1.
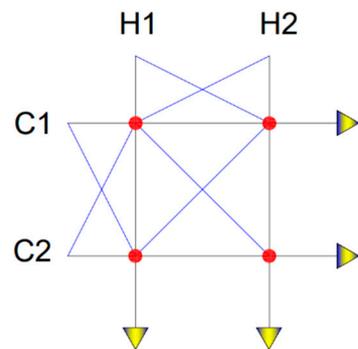
Figure 3. Graphical structure expression of submatrix A.
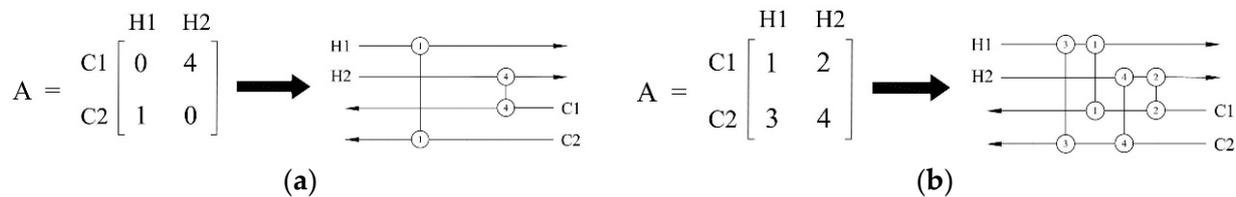
Figure 4. Two structure representations of submatrix A in the case of four streams: (**a**) structure representation 1; (**b**) structure representation 2.

By defining submatrix A, a HEN is characterized without considering the utility supply, which is taken into account in submatrices B and C.

2.1.2. Submatrix B (Hot Utility Matrix)

The number of columns in submatrix B is 1, and the number of rows is equal to the number of cold streams. The matrix element b_j is a binary variable, with 0 showing that the cold stream does not require hot utilities and 1 showing that the cold stream requires additional hot utilities.

2.1.3. Submatrix C (Cold Utility Matrix)

The number of rows in submatrix C is 1, and the number of columns is equal to the number of hot streams. The matrix element c_i is a binary variable, with 0 showing that the hot stream does not require cold utilities and 1 showing that the hot stream requires additional cold utilities.

2.1.4. Submatrix D (Zero Matrix)

Submatrix D is a zero matrix with a matrix element count of one since no heat exchange is required between the hot utility and the cold utility.

2.2. Objective Function

The objective function is the total annualized capital costs (*CC*) and utility expenses for process heat exchangers (*UC*). The purpose is to reduce the so-called total annual cost (*TAC*). At a process plant, the HEN needs to be enhanced to recover the useful energy between the streams as inexpensively as feasible, since the investment in heat exchange equipment is unavoidable, in order to minimize the energy consumption of utilities. Equation (3) may be used to compute the trade-off between operating cost and investment cost, which determines the HEN's overall yearly cost:

$$TAC = CC + UC \tag{3}$$

2.2.1. Capital Cost

The capital cost (*CC*) of the HEN includes the manufacturing expenses of the heat exchanger area and the fixed charge of the heat exchanger. With the consideration of individual heat exchanger areas A in m^2 and three coefficients C_F, C_A, and β (Equation (4)), the specification of heat exchanger costs in the case studies reported in this work may be defined based on a common potential approach [8],

$$CC = \sum_{i=1}^{i} \sum_{N=1}^{N} (C_F \times Z_{i,N} + C_A \times A_{i,N}^{\beta}) \tag{4}$$

where $Z_{i,N}$ is an integer variable representing whether the heat unit exists ($Z_{i,N} = 1$) or not ($Z_{i,N} = 0$). The area of heat exchange *A* is calculated as follows:

$$A_{i,j} = \frac{Q_{i,j}}{(K_{i,j} \times LMTD_{i,j})} \tag{5}$$

where *Q* denotes the load of the heat exchanger, *K* is the heat transfer coefficient, *LMTD* is the logarithmic mean temperature difference, and the subscripts *i* and *j* indicate hot stream and cold stream, respectively.

Without considering the thermal resistance of the heat-exchanging surface, the simplified total heat transfer coefficient is estimated. Equation (6), where *h* is the unique heat exchange coefficient of streams, calculates the total heat exchange coefficient *K*,

$$K_{i,j} = \frac{h_i h_j}{(h_i + h_j)} \tag{6}$$

The temperature difference is typically determined using the logarithmic mean temperature difference (*LMTD*) formula (Equation (7)). However, the arithmetic mean temperature difference (*AMTD*) is utilized (Equation (8)) when the temperature differences between the heat exchanger's two ends are equal. Here, $T_{h,i,j}^{in}$ and $T_{h,i,j}^{out}$ are inlet and outlet temperatures of a single exchanger for a hot stream; $T_{c,i,j}^{in}$ and $T_{c,i,j}^{out}$ are inlet and outlet temperatures of a single exchanger for a cold stream,

$$LMTD_{i,j} = \frac{\theta_1 - \theta_2}{ln(\theta_1/\theta_2)} \tag{7}$$

$$AMTD_{i,j} = \frac{\theta_1 + \theta_2}{2} \tag{8}$$

$$\theta_1 = T_{h,i,j}^{in} - T_{c,i,j}^{out} \tag{9}$$

$$\theta_2 = T_{h,i,j}^{out} - T_{c,i,j}^{in} \tag{10}$$

2.2.2. Utility Cost

Equation (10)—in which C_{CU} and C_{HU} are the unit operation costs of cold and hot utilities, respectively, and qCU_i and qHU_j represent the cold utility load on the *i*th hot stream and the hot utility load on the *j*th cold stream, respectively—demonstrates the objective function of utility cost (*UC*), which includes consumption costs of the hot utility and cold utility,

$$UC = C_{CU} \times \sum_{i=1}^{i} qCU_I + C_{HU} \times \sum_{j=1}^{j} qHU_J \tag{11}$$

2.3. Constraints

The network streams guarantee heat conservation and conform to engineering applications by the HEN constraints.

2.3.1. Overall Heat Balance for Each Stream

Overall heat balance for each stream ensures that the cold and hot streams can reach the target temperature.

$$(T_i^{IN} - T_i^{OUT})FCp_i = \sum_{j=1}^{j} Q_{i,j} + Q_{CU,i} \tag{12}$$

$$(T_j^{OUT} - T_j^{IN})FCp_j = \sum_{i=1}^{i} Q_{i,j} + Q_{HU,j} \tag{13}$$

where T_i^{IN} and T_i^{OUT} are the inlet and target temperatures of hot streams; T_j^{IN} and T_j^{OUT} are the inlet and target temperatures of cold streams; and FCp_i and FCp_j are heat capacity flow rates of hot and cold streams.

2.3.2. Heat Balance of Each Heat Exchanger

Heat balance of each heat exchanger is used to calculate the outlet tempera-ture of the heat exchanger for hot and cold streams, and to ensure the conservation of heat.

$$Q_{i,j} = (T_{h,i,j}^{in} - T_{h,i,j}^{out})FCp_i = (T_{c,i,j}^{out} - T_{c,i,j}^{in})FCp_j \tag{14}$$

2.3.3. Heat Balance for the Utility at Stream End

The utilities ensure that the cold and heat streams reaches the target temperature.

$$(T_i^{out} - T_i^{OUT})FCp_i = Q_{CU,i} \tag{15}$$

$$(T_j^{OUT} - T_j^{out})FCp_j = Q_{HU,j} \tag{16}$$

Equation (14) can be used to calculate the temperatures of the hot and cold streams' terminal outlets (T_i^{out} and T_j^{out}) from the inlets of each stream using the structures and heat distribution that are provided.

2.3.4. Temperature Feasibility Constraints for Each Stream

Temperature feasibility constraints for each stream is used to ensure that the temperature of the streams always keeps monotonically increasing or decreasing.

$$T_{h,i,j,a_1}^{out} \geq T_{h,i,j,a_2}^{out} \tag{17}$$

$$T_{c,i,j,a_1}^{out} \leq T_{c,i,j,a_2}^{out} \tag{18}$$

$$T_{h,i,j}^{out} \geq T_i^{out} \geq T_i^{OUT} \tag{19}$$

$$T_{c,i,j}^{out} \leq T_j^{out} \leq T_j^{OUT} \tag{20}$$

where the elements a_1 and a_2 of submatrix A are on the same stream, and a_1 is greater than a_2. The temperature of the hot stream progressively decreases, and the temperature of the cold stream gradually increases throughout the computation of each inlet and output temperature for each heat exchanger as indicated above.

2.3.5. Minimum Temperature Approach Constraints

Minimum temperature approach constraints are used to ensure that the heat exchange network meets the engineering application, but also to avoid excessive area of heat exchange.

$$T_{h,i,j}^{in} - T_{c,i,j}^{out} \geq \Delta T_{min} \tag{21}$$

$$T_{h,i,j}^{out} - T_{c,i,j}^{in} \geq \Delta T_{min} \tag{22}$$

$$T_i^{out} - T_{CU}^{out} \geq \Delta T_{min} \tag{23}$$

$$T_i^{OUT} - T_{CU}^{in} \geq \Delta T_{min} \tag{24}$$

$$T_{HU}^{in} - T_j^{OUT} \geq \Delta T_{min} \tag{25}$$

$$T_{HU}^{out} - T_j^{out} \geq \Delta T_{min} \tag{26}$$

where ΔT_{min} is the program's minimal approach temperature setting for the network. Here, T_{CU}^{in} and T_{CU}^{out} denote the inlet and outlet temperatures of the cold utility, respectively. The corresponding symbols for the hot utility are T_{HU}^{in} and T_{HU}^{out}.

2.3.6. Matrix Element Constraints

① Non-negativity constraints:

$$a_{ij} \geq 0 \tag{27}$$

$$b_j \geq 0 \tag{28}$$

$$c_i \geq 0 \tag{29}$$

② Uniqueness constraint:

In submatrix A, the matrix element a_{ij} represents whether the heat exchanger exists as well as the matching order among streams. Therefore, a_{ij} is unique when a_{ij} is not zero. The expression form of a_{ij} is shown following Equation (2).

2.3.7. Target Temperature Accuracy Constraint

The hot and cold streams' respective accuracy requirements for target temperatures are

$$abs(T_i^{out} - T_i^{OUT}) \leq AD \, n \in N_H \tag{30}$$

$$abs(T_j^{out} - T_j^{OUT}) \leq AD \, n \in N_C \tag{31}$$

where *AD* is the acceptable deviation of the hot and cold streams' target temperature.

3. Solution Algorithm

The genetic algorithm (GA) was proposed by Holland in 1975 based on the principle of survival of the fittest. It is widely used in the field of optimization. The initialized population, fitness value evaluation, selection, crossover, and mutation phases make up the core of the GA, and the loop iteration method is used to reach the best result. The GA can be individually applied to the optimization problem of a mixed integer HEN; it can also be combined with other optimization algorithms to complete the optimization. The induction of the elitist preservation strategy, for which the best individual of each generation can be preserved, avoids crossover and mutation in the operating loss of the global optimal solution.

3.1. Matrix Real-Coded Genetic Algorithm

The encoding method of genetic algorithms determines the calculation method and efficiency of population genetics. In this paper, the matrix real-coded form is adopted according to the structure of the mathematical matrix. The definition of the M-NSM allows a more flexible and straightforward representation of individual situations within a broader feasible region. The matrix coding genetic algorithm can not only keep the flexibility of the binary coding crossover and mutation, but it is also suitable for matrix optimization. The matrix real-coded form used in this genetic algorithm is the same as the expression of the structural variable of the M-NSM model; that is, the individuals encoded by the real number of the matrix carry the semantic information of the structure. The solution space is used as the genotype, which requires no decoding and is more efficient, and the data structure of the matrix real-coded form has a larger expression space. In the M-NSM, submatrix A is the key submatrix, and submatrix B and submatrix C are determined by submatrix A. Thus, the whole optimization process of the elitist genetic algorithm (EGA) is completed in submatrix A.

3.1.1. Initialization

The initialization of the optimization variables is performed at random to find the individuals. Each individual in this population represents a potential fix for a problem. According to the fitness function, each individual is assessed and given a fitness value. For a HEN with M hot streams and N cold streams, an $(M + 1) \times (N + 1)$ matrix is used as a genotype, where submatrix A is an $M \times N$ matrix that is randomly generated when the population is initialized. The size of individual populations needs to be adjusted according to the number of streams. A small population is easy to converge; a large population is difficult to converge, and the robustness decreases.

3.1.2. Fitness Function

The selection of the fitness function is the key factor in genetic algorithms since it can affect the population's results. In this paper, the total annual cost is chosen as the fitness function.

3.1.3. Selection

According to the fitness value of each chromosome, selection is a random process that chooses a parent chromosome from a population. Due to its simplicity and effectiveness in algorithm execution, the tournament selection algorithm is a highly common selection technique in genetic algorithms. The population is chosen for the tournament by a pre-determined number, with the fittest individuals moving on to the next generation. This selection procedure is carried out repeatedly until the population size is reached in the next generation.

3.1.4. Crossover

A crossover in the EGA is a stochastic search operator that creates an individual offspring from one generation to the next. Earlier studies have demonstrated that the

evolutionary approach using binary-coded GAs is effective when using the binary crossover (BX), which is employed to generate individuals. As a result, the simulated binary crossover (SBX), which is based on an observed probability distribution applied to a real-coded domain, was developed to perform the operation of BX [19]. The idea behind the SBX is to mimic the properties of the single-point crossover typically used by binary-coded chromosomes. One of these properties is that the average of the parents is equal to the average of the offspring. Generally, the crossover probability ranges from 0.4 to 0.99. A small crossover probability is not conducive to population renewal, while a large crossover probability will destroy the favorable population model and increase the randomness.

3.1.5. Mutation

In genetic algorithm chromosomes, the mutation is employed to preserve genetic variety from one population generation to the next generation. Considering the actual meaning represented by the matrix and avoiding the duplication of matrix elements in submatrix A, two matrix elements a_1 and a_2 in submatrix A are randomly selected to exchange location during the mutation, and other positions remain unchanged. The gene mutation operation demonstration is shown in Figure 5. Although the mutation only exchanges the location of two matrix elements, it changes the matching order of the entire network of streams, so the HEN structure will change accordingly. Generally, the mutation probability is 0.0001~0.1. If the mutation probability is too small, the population diversity will decline too fast, and the effective gene will be easily lost.
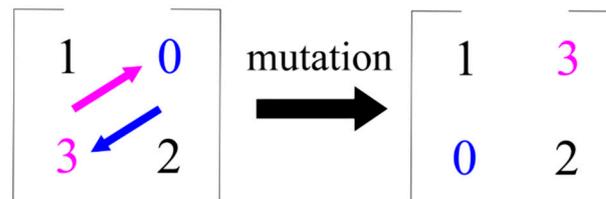
Figure 5. Demonstration of submatrix A gene mutation.

3.1.6. Elitist Preservation Strategy

The core idea of the elitist preservation strategy is to replicate the elite individuals that appear in the process of population evolution to the next generation. Elite individuals are individuals with the best fitness value in population evolution, and they contain the best genetic data at present. The elitist preservation strategy effectively improves the convergence ability of the algorithm.

3.2. Solution Strategy

The HEN model is solved using an effective two-stage optimization technique [20], where the first level uses EGA to address network topologies related to integer variables and the second level uses a binary search to tackle heat loads related to continuous variables. In other words, one level corresponds to the topology of the HEN, and the other level corresponds to the load distribution under a given topology. The study demonstrates that using two-level approaches somewhat enhances HEN outcomes [18].

Due to the process of initialization and population evolution, there will be a large number of infeasible HEN structures. In order to control the solution complexity of the M-NSM efficiently and improve its solving efficiency, the structural repair strategy is considered at the topological level. The structural repair strategy is used to verify the matching of the streams in submatrix A according to the order of the matrix elements a_{ij}. The matrix elements of the current position are set to 0 if the constraints are not met. Heat load optimization can be achieved for a given topology after the HEN structure has been repaired. Heat load distribution at this level is similar to the "tick-off" idea in pinch point technology on the premise of satisfying the ΔT_{min} to find the maximum heat loads for stream matching under the current situation. The use of a "tick-off" to ensure the

design is steered towards the fewest possible units and the solution of the "remaining stream matching problem" [21]. Because the search range of heat loads is an ordered and continuous interval, the binary search is employed. The design of process heat exchangers inevitably affects the heat loads of utility heat exchangers. The calculation scheme is given in Figure 6.
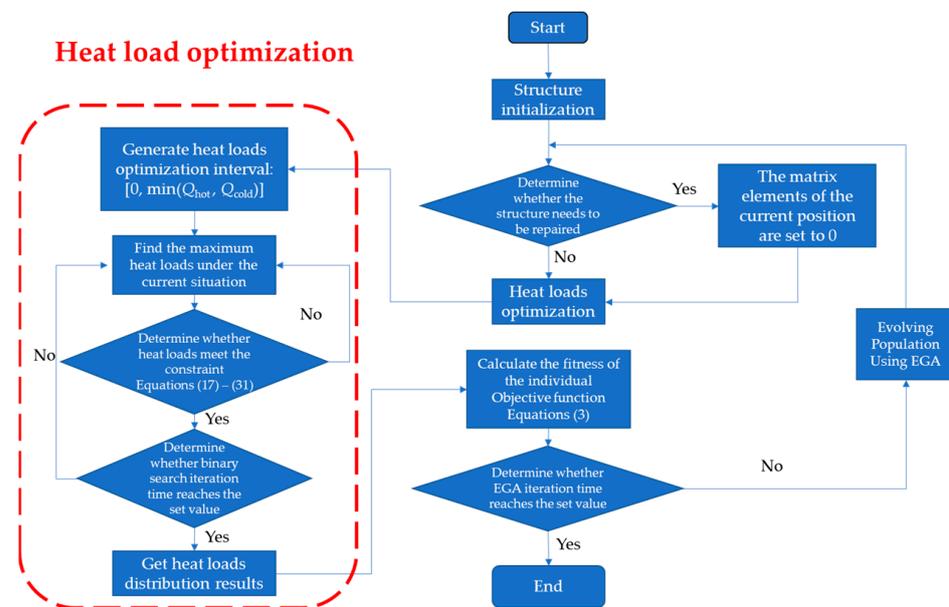
Figure 6. Calculation scheme of two-level optimization algorithm.

The following steps describe the two-level optimization process for finding a workable solution:

Step 1: Obtain the program's stream and cost data. Provide the maximum number of binary searches and EGA iterations. Create a specified number of individuals with arbitrary chromosomal distributions and a single HEN structure for each of them [22].

Step 2: Determine whether the individual HEN structure needs to be repaired according to the constraint Equations (17)–(26). If necessary, execute the structure repair strategy to repair the individual HEN structure; otherwise, the scheme goes to Step 3.

Step 3: Generate the heat load optimization interval of process heat exchangers: $[0, \min(Q_{hot}, Q_{cold})]$. The optimization interval ranges from 0 to the value with the fewest heat loads required in the hot stream and cold stream.

Step 4: Optimize heat loads of process heat exchangers similar to the tick-off idea of pinch point technology on the premise of satisfying the ΔT_{min} and the constraint Equations (17)–(31) to find the maximum heat loads for streams matching under current situation.

Step 5: Determine whether the number of binary search iteration times reaches the set value; if not, the scheme goes back to Step 4 and otherwise goes to the next steps.

Step 6: Calculate the fitness of the individual (objective function Equation (3)) and save the best individual with the highest fitness as an elite individual.

Step 7: Determine whether the number of EGA iteration times reaches the set value; if not, the scheme goes to the next steps and otherwise goes to last step.

Step 8: According to the fitness value, obtain the new population by the selection method of the tournament combined with the elitist preservation strategy. Then, conduct crossover and mutation between the individuals in the population to obtain the next generation population. Return to Step 2 after the evolution.

Step 9: Repeat the above steps until the set EGA iteration time is reached, and output the optimal result.

4. Case Studies and Discussion

The proposed M-NSM was used to solve three HEN problems of various sizes using a two-level optimization approach. The cases have already been resolved by several authors using a range of methods. When compared to other approaches described in the literature, the optimal results of the cases demonstrate the viability and effectiveness of the M-NSM. Using a Windows Server system powered by an Intel(R) Core (TM) Processor i7-10710U @ 1.1 GHz, the code was developed using Spyder (Python 3.8).

4.1. Case Study 1

Ahmad [23] first suggested the ten-stream problem in this case, and other academics have adopted it as a benchmark [23]. The process data are summarized in Table 1. In contrast to other cases, this case does not require fixed heat exchanger charges, and since the area exponent is 1, the number of heat exchangers might expand indefinitely if the streams are well matched [15]. The added heat exchanger will not result in additional cost. As a result, the performance of the matrix non-structural model is evaluated using this unique example.

Table 1. Problem data for case study 1.

Stream	T^{IN} (°C)	T^{OUT} (°C)	FCp (KW/K)
H1	85	45	156.3
H2	120	40	50.0
H3	125	35	23.9
H4	56	46	1250.0
H5	90	86	1500.0
H6	225	75	50.0
C1	40	55	466.7
C2	55	65	600.0
C3	65	165	180.0
C4	10	170	81.3
Hot utility	200	198	-
Cold utility	15	20	-

$K = 0.025$ KW/(m^{2}K) for all matches.
Annual cost of heat exchangers = $60A$ \$/year (A in m^2).
Annual cost of hot utility = 100 \$/kW year.
Annual cost of cold utility = 15 \$/kW year.

In this case, the population size is chosen randomly to be 100, the number of iterations is 200, the acceptable deviation of the target temperature is 0.001, the rate of crossover is 0.9, and the rate of mutation is 0.1. The evolution of the optimum solution in the EGA for case study 1 is shown in Figure 7. After 19 s, the best solution was found with an annual cost of \$5,649,631. According to Figure 8, the ideal HEN structure comprises 15 units. The heat exchangers' fixed expenses were not considered in the first supposition. The HEN structure becomes more complex, and the cost-optimal solution is represented by HEN systems with numerous heat exchanger units. This is because no fixed costs are assumed. The HEN in the existing solution with stream splits is more complicated than the HEN without stream splits, and the cost of the extra pipeline and the accessories required for the stream split has not been taken into account. Several researchers have utilized the data presented in Table 1 as a standard, and Table 2 compares various solutions. Compared with the results obtained by Ahmad [23], the case based on the M-NSM in this paper has a great economic advantage. Compared with the subsequent optimization scheme, it better balances the structural complexity of the HEN and the total annual cost. Furthermore, the result in this paper requires minimal heat and cold utilities, reducing energy consumption.
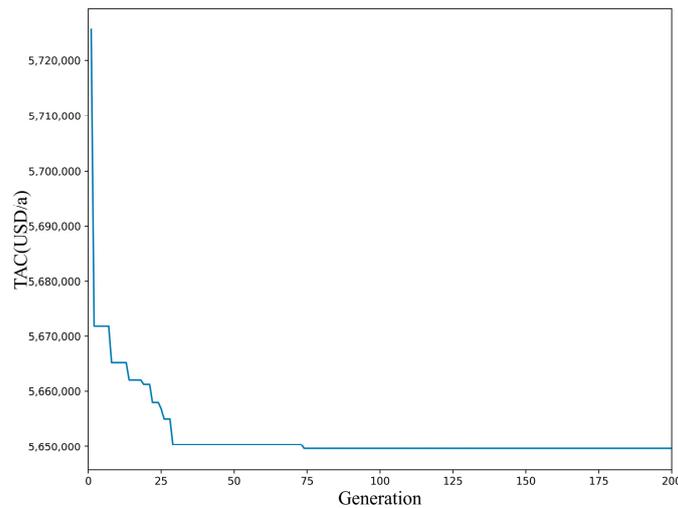
Figure 7. Evolution of the best solution in the EGA in case study 1.
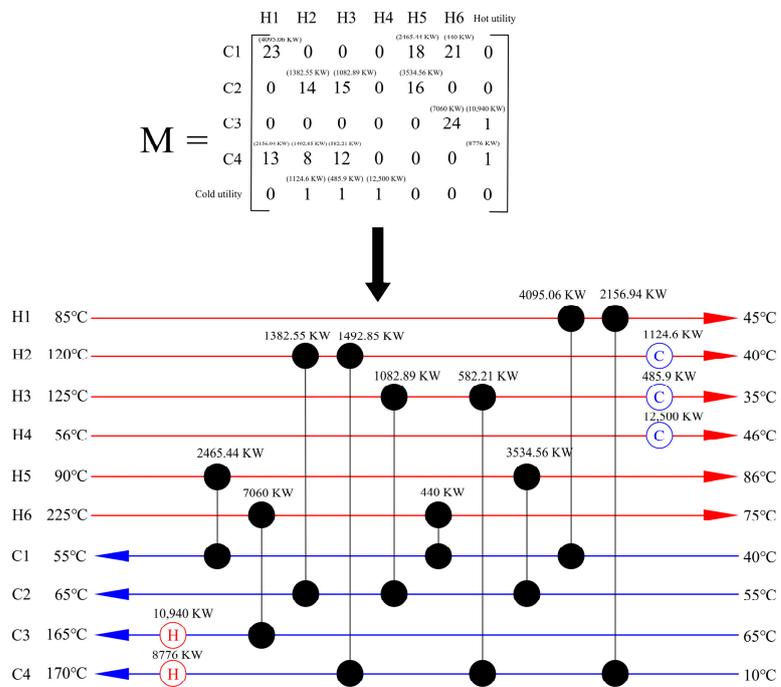
Figure 8. Optimal results for case study 1; *TAC* = 5,649,631 $/year.

Table 2. Results comparison for case study 1.

Method	Units	Q_{HU} (KW)	Q_{CU} (KW)	*TAC* ($/year)
Ahmad [23]	-	15,400	9796	7,074,000
Ravagnani et al. [24]	13	20,529.3	14,923.8	5,672,821
Yerramsetty and Murty [25]	13	20,745.4	15,139.9	5,666,756
Huo et al. [26]	13	19,991	14,385	5,657,000
Peng and Cui [27]	18	20,399	14,733.5	5,609,271
Zhang et al. [15]	19	20,276	14,670.5	5,607,762
Chen and Cui [28]	24	20,396	14,790.5	5,593,970
This study (Figure 8)	15	19,716	14,110.5	5,649,631

Based on the analysis and results of case study 1, the proposed method can be validated by the benchmark HEN problem, with its *TAC* being competitive with other methods.

4.2. Case Study 2

The second case represents a nitric acid plant, which was first studied by Castillo et al. [29]. The decrease in carbon emissions and expenses was achieved by the authors using pinch analysis. In this case, there are six hot and five cold streams, and the statistics are given in Table 3. Comparing the results of several algorithms reveals that the majority of cost-optimal results fall in the region of about 139,000 \$/year [8]. Matthias Rathjens and Georg Fieg published the best solution so far, with 11 heat-exchanging units [8].

Table 3. Problem data for case study 2.

Stream	T^{IN} (K)	T^{OUT} (K)	FCp (KW/K)	H (KW/m^{2}K)
H1	1113	313	4.9894	1.5
H2	349	318	4.6840	1.5
H3	323	313	0.772	1.5
H4	453	350	0.6097	1.5
H5	453	452	292.7	0.8
H6	363	318	3.066	1.5
C1	297	298	329.8	0.8
C2	298	343	0.5383	1.5
C3	308	395	3.727	1.5
C4	363	453	0.6097	1.5
C5	453	454	2581.1	0.8
Hot utility	503	503	-	1.5
Cold utility	293	313	-	0.8

Annual cost of heat exchangers = $9094 + 485A^{0.81}$ \$/year (A in m^2).
Annual cost of hot utility = 110 \$/kW year.
Annual cost of cold utility = 15 \$/kW year.

In this case, the population size is chosen randomly as 100, the number of iterations is 200, the rate of crossover is 0.9, and the rate of mutation is 0.1. After calculation, it is found that the HEN structure of case 2 is closely related to the setting of AD. When AD is set to 0.01 and 0.001, two better HEN structures can be obtained, respectively. It is noteworthy that the HEN structure with just 10 heat exchangers when AD is 0.01 is simpler than those described by other researchers, and that the total annual cost of this configuration is, likewise, less than the lowest recorded cost in the literature.

The iteration process is shown in Figures 9 and 10. The optimization results for case 2 with AD of 0.01 and 0.001 are illustrated in Figures 11 and 12, respectively. Their computation times are less than 9 s and 10 s. Comparing the two HEN structures in Figures 11 and 12, the structure of submatrix A of the two HEN structures is consistent, and there is only a difference in the number of coolers. The matching heat loads of H5 and C1 in the two HEN structures are both 291.22KW, but in fact, it takes 292.7KW for H5 to reach the target temperature. After heat exchange with C1, the final temperature of H5 is 452.005 °C, which is only 0.005 °C different than its target temperature of 452 °C. When AD is 0.01 °C because 0.005 °C < 0.01 °C (AD), we assume that the heat exchange has been completed by H5, and no additional cold utility is needed; thus, one cooler will be saved compared to other solutions. Table 4 shows the details of the obtained HEN compared to those found in the literature. With the HEN structure shown in Figure 11, a simpler solution is achieved with lower *TAC* (\$130,877/year) and no stream splits. This indicates that the configuration is more advantageous in terms of overall HEN investments, piping complexity, and costs. It is also important to note that the total amount of cold utilities used by the HEN described in all the published work so far is almost equal. It can be said that the two solutions identified by the current methodology are better equipped to disperse heat loads across the HEN in order to decrease the total area needed to complete the same activity since they have lower *TAC*.
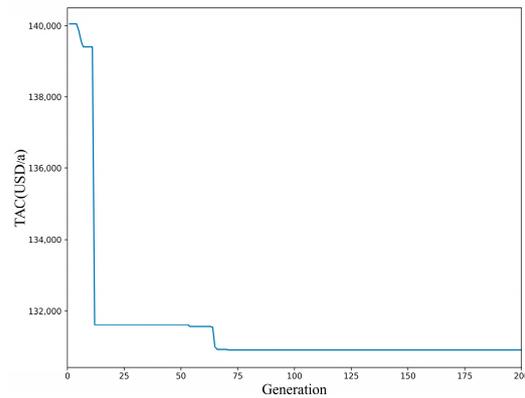
Figure 9. Evolution of the best solution in the EGA in case study 2. (AD = 0.01 °C).
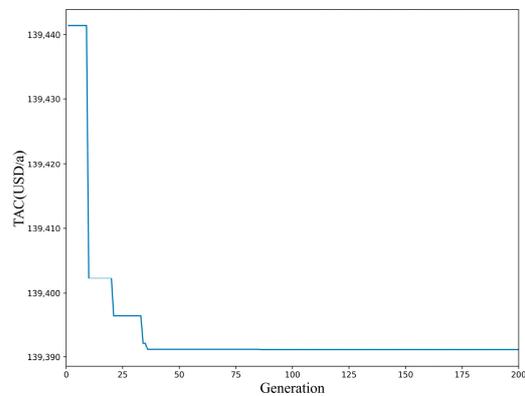
Figure 10. Evolution of the best solution in the EGA in case study 2. (AD = 0.001 °C).
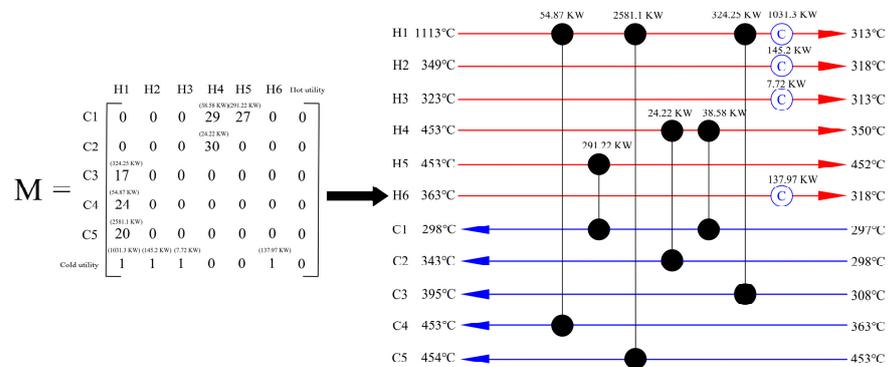
Figure 11. Optimal results for case study 2; *TAC* = 130,877 $/year. (AD = 0.01 °C).
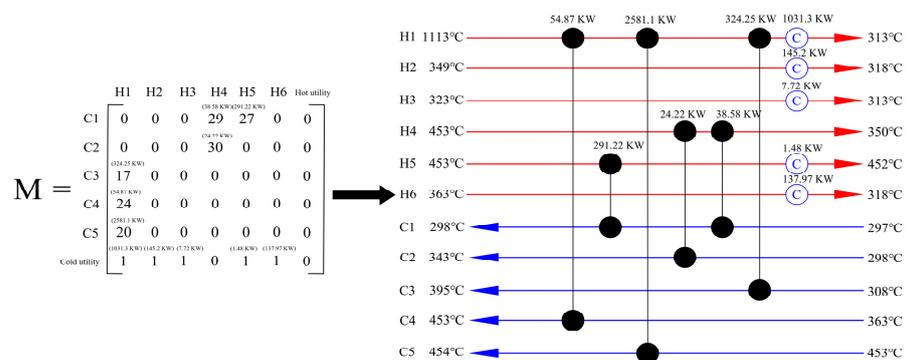
Figure 12. Optimal results for case study 2; *TAC* = 139,391 $/year. (AD = 0.001 °C).

Table 4. Results comparison for case study 2.

Method	Units	Q_{HU} (KW)	Q_{CU} (KW)	*TAC* ($/year)
Castillo et al. [29]	11	0	1323.67	141,554
Silva et al. [30]	11	0	1323.67	140,141
Pavão et al. [22]	11	0	1323.67	140,068
Pavão et al. [31]	11	0.33	1324	139,438
Aguitoni et al. [32]	11	0	1323.66	139,616
Rathjens and Fieg [8]	11	0	1323.67	139,387
This study (Figure 11)	10	0	1322.19	130,877
This study (Figure 12)	11	0	1323.67	139,391

4.3. Case Study 3

Björk and Pettersson's case study was used for the third example [33]. It has seven cold streams and eight hot streams. Table 5 shows the pertinent information. Table 6 compares findings from the literature [27,33–38]. Recently, this case study attracted a lot of attention [8]. Björk and Pettersson [33] altered the stage-wise superstructure model and permitted stream splits. Although Björk and Pettersson's initial solution [33] was already quite competitive, the optimal structures and computational time were not offered. In addition, most current solutions require a few hundred hours of computational time, which may not follow our definition of a reasonable computation time. The motivation of this paper is to test the performance of the M-NSM that can find satisfactory network designs with satisfactory computational time. Furthermore, as the complexity of the network's components also has a significant impact on HEN performance, *TAC* reductions should not be the only goal. Therefore, a HEN without stream splits has certain advantages over a HEN with stream splits in terms of structural stability and construction difficulty.

Table 5. Problem data for case study 3.

Stream	T^{IN} (°C)	T^{OUT} (°C)	*FCp* (KW/K)	*h* (KW/m²K)
H1	180	75	30	2
H2	280	120	60	1
H3	180	75	30	2
H4	140	40	30	1
H5	220	120	50	1
H6	180	55	35	2
H7	200	60	30	0.4
H8	120	40	100	0.5
C1	40	230	20	1
C2	100	220	60	1
C3	40	190	35	2
C4	50	190	30	2
C5	50	250	60	2
C6	90	190	50	1
C7	160	250	60	3
Hot utility	325	325	-	1
Cold utility	25	40	-	2

Annual cost of heat exchangers = $8000 + 500A^{0.75}$ $/year (*A* in m²).
Annual cost of hot utility = 80 $/kW year.
Annual cost of cold utility = 10 $/kW year.

In this case, the population size is chosen randomly to be 300, the number of iterations is 300, the acceptable deviation of target temperature is 0.001, the rate of crossover is 0.9, and the rate of mutation is 0.1. The iteration process can be found in Figure 13. The optimization result within 89 s of computation time is shown in Figure 14. In comparison to the advancements achieved over the years for cost optimization in this case study, the result gives a lower *TAC* (1,524,564 $/year) with much less computational time. Therefore,

case study 3 also proves that the combined application of the two-level method and the M-NSM improves the computational efficiency and results of the HEN.

Table 6. Results comparison for case study 3.

Method	Units	Q_{HU} (KW)	Q_{CU} (KW)	*TAC* ($/year)
Björk and Pettersson [33]	-	-	-	1,513,854
Björk and Nordman [34]	-	-	-	1,530,063
Hu et al. [35]	22	-	-	1,568,981
Chen and Luo [36]	21	-	-	1,549,979
Peng and Cui [27]	17	10,974	8599	1,537,252
Chen and Luo [37]	21	10,255	7880	1,534,642
Peng and Cui [27]	19	10,109	7734	1,527,240
Pavão et al. [38]	19	-	-	1,525,394
This study (Figure 14)	20	10,393	8018	1,524,564
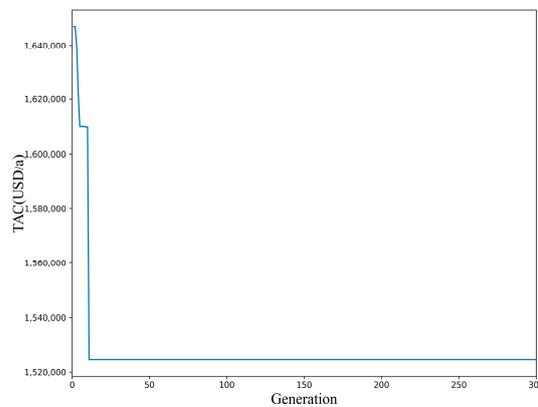
Figure 13. Evolution of the best solution in the EGA in case study 3.
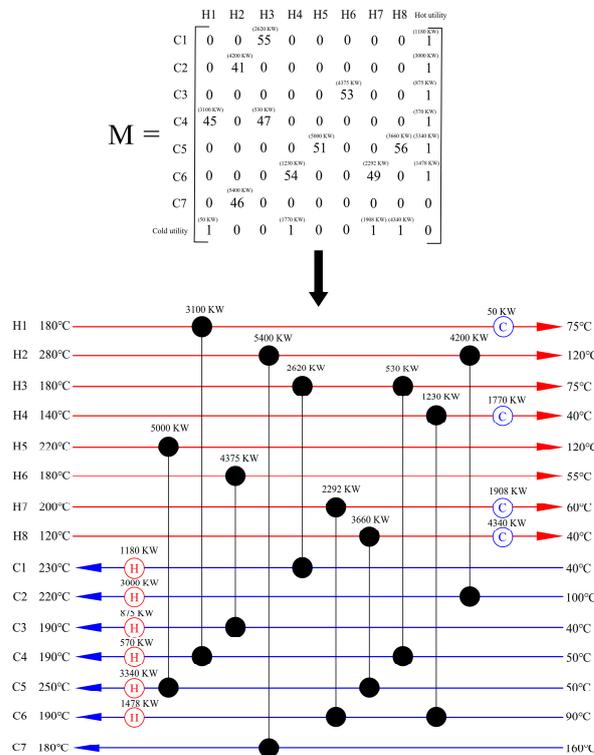
Figure 14. Optimal results for case study 3; *TAC* = 1,524,564 $/year.

5. Conclusions

The aim of this paper is to develop a novel M-NSM for the HEN without stream splits from the perspectives of global optimization methods and superstructure models. In the proposed M-NSM, the heat exchanger position order is quantized by matrix elements at each stream. The M-NSM without stages divided has a wide range of expansibility, in addition to an uncomplicated, clear visual impression. In order to control the solution complexity of the M-NSM efficiently and improve its the solving efficiency, the EGA and structural repair strategy are used at the topological level. For the load distribution for a given topology, heat loads of process heat exchangers are optimized, similarly to the tick-off idea in pinch point technology. The synthesis performance of the M-NSM has been demonstrated using three case studies. *TAC* in case study 1 is reduced by 20.13% compared to the original scheme. The M-NSM model balances the number of heat exchangers and *TAC* well compared to other schemes. In case study 2, when AD = 0.01 °C, the optimal scheme with the lowest number of heat exchangers is obtained, and *TAC* is 6.11% less than the optimal scheme of Rathjens. In case study 3, the computational results show that the M-NSM balances the solution result and computational efficiency well and can find economical networks with no splits within a reasonable computational time. As demonstrated in this paper, the suggested method is a good replacement for traditional HEN synthesis techniques and has a good potential for resolving practical, industrial-scale HEN synthesis issues.

Nomenclature

A	area of heat exchange
a_{ij}	multivariate matrix element in submatrix A
AD	acceptable deviation of the stream target temperature
AMTD	arithmetic mean temperature difference
b_j	matrix element in submatrix B
C_A	coefficient of area cost
C_{CU}	unit operation cost of cold utility
C_F	fixed capital cost
C_{HU}	unit operation cost of hot utility
c_i	matrix element in submatrix C
CC	capital cost of the HEN
FCp	heat capacity flow rates of stream
h	individual heat exchange coefficient of streams
K	overall heat exchange coefficient
LMTD	logarithmic mean temperature difference
Q	heat load
Q_{CU}	cold utilities
Q_{HU}	hot utilities
qCU	cold utility load on the hot stream
qHU	hot utility load on the cold stream

T^{IN}	inlet temperature of stream
T^{in}	inlet temperatures of a single exchanger for stream
T^{OUT}	target temperature of stream
T^{out}	outlet temperatures of a single exchanger for stream
TAC	total annual cost
UC	utility cost
$Z_{i,N}$	an integer variable representing whether the heat unit exists or not
ΔT_{min}	minimum approach temperature preset for the network
θ_1	approach temperature at hot end of the heat exchanger
θ_2	approach temperature at cold end of the heat exchanger
Subscripts	
CU	cold utilities
HU	hot utilities
i	cold stream
j	hot stream
Superscripts	
β	area cost exponent

References

1. Xiao, Y. Global Optimization Methods and Superstructure Model for Heat Integration of Heat Exchanger Networks. Ph.D. Dissertation, University of Shanghai for Science and Technology, Shanghai, China, 2018.
2. Brandt, C.; Fieg, G.; Luo, X. Efficient synthesis of heat exchanger networks combining heuristic approaches with a genetic algorithm. *Heat Mass Transf.* **2011**, *47*, 1019–1026. [CrossRef]
3. Linnhoff, B.; Hindmarsh, E. The pinch design method for heat exchanger networks. *Chem. Eng. Sci.* **1983**, *38*, 745–763. [CrossRef]
4. Zhao, Y.; Sun, L.; Luo, X. Research advances in pinch technology and the synthesis of multipass heat exchanger networks. *Chem. Ind. Eng. Prog.* **2012**, *31*, 1685–1689.
5. Kemp, I.C. *Pinch Analysis and Process Integration*; Butterworth-Heinemann (Elsevier): Oxford, UK, 2007; pp. 99–159. [CrossRef]
6. Xu, Y.; Cui, G.; Han, X.; Xiao, Y.; Zhang, G. Optimization route arrangement: A new concept to achieve high efficiency and quality in heat exchanger network synthesis. *Int. J. Heat Mass Transf.* **2021**, *178*, 121622. [CrossRef]
7. Cerda, J.; Westerburg, A.W. Synthesizing heat exchanger networks having restricted stream/stream matches using transportation problem formulations. *Chem. Eng. Sci.* **1983**, *38*, 1723–1740. [CrossRef]
8. Rathjens, M.; Fieg, G. A novel hybrid strategy for cost-optimal heat exchanger network synthesis suited for large-scale problems. *Appl. Therm. Eng.* **2020**, *167*, 114771. [CrossRef]
9. Floudas, C.; Grossmann, I. Synthesis of flexible heat exchanger networks with uncertain flowrates and temperatures. *Comput. Chem. Eng.* **1987**, *11*, 319–336. [CrossRef]
10. Floudas, C.A.; Grossmann, I.E. Automatic generation of multiperiod heat exchanger network configurations. *Comput. Chem. Eng.* **1987**, *11*, 123–142. [CrossRef]
11. Grossmann, I.; Floudas, C. Active constraint strategy for flexibility analysis in chemical processes. *Comput. Chem. Eng.* **1987**, *11*, 675–693. [CrossRef]
12. Huang, K.F.; Karimi, I.A. Simultaneous synthesis approaches for cost-effective heat exchanger networks. *Chem. Eng. Sci.* **2013**, *98*, 231–245. [CrossRef]
13. Smith, R.; Jobson, M.; Chen, L. Recent development in the retrofit of heat exchanger networks. *Appl. Therm. Eng.* **2010**, *30*, 2281–2289. [CrossRef]
14. Lu, Z.; Cui, G.; Zhang, Q.; Gao, X. Application of chessboard model in heat exchanger networks optimization. *Chem. Eng.* **2007**, *35*, 16–19.
15. Zhang, H.; Cui, G.; Xiao, Y.; Chen, J. A novel simultaneous optimization model with efficient stream arrangement for heat exchanger network synthesis. *Appl. Therm. Eng.* **2017**, *110*, 1659–1673. [CrossRef]
16. Zamora, J.M.; Grossmann, I.E. A global MINLP optimization algorithm for the synthesis of heat exchanger networks with no stream splits. *Comput. Chem. Eng.* **1998**, *22*, 367–384. [CrossRef]
17. Khorasany, R.M.; Fesanghary, M. A novel approach for synthesis of cost-optimal heat exchanger networks. *Comput. Chem. Eng.* **2009**, *33*, 1363–1370. [CrossRef]
18. Chen, J.; Yang, Q.; Cui, G.; Bao, Z.; Zhang, G. Synthesis of Cost-Optimal Heat Exchanger Networks Using a Novel Stochastic Algorithm and a Modified Stage-Wised Superstructure. *Processes* **2021**, *9*, 2060. [CrossRef]
19. Lin, J.-J.; Huang, S.-C.; Jiau, M.-K. An Evolutionary Multiobjective Carpool Algorithm Using Set-Based Operator Based on Simulated Binary Crossover. *IEEE Trans. Cybern.* **2018**, *49*, 3432–3442. [CrossRef]
20. Lewin, D.R. A generalized method for HEN synthesis using stochastic optimization—II: The synthesis of cost-optimal networks. *Comput. Chem. Eng.* **1998**, *22*, 1387–1405. [CrossRef]
21. Zhang, W.; Sun, W.; Liu, J. *Analysis and Synthesis for Chemical Engineering Process*; Chemical Industry Press: Beijing, China, 2011; pp. 197–212.

22. Pavão, L.V.; Costa, C.B.B.; Ravagnani, M.A.D.S.S. Automated heat exchanger network synthesis by using hybrid natural algorithms and parallel processing. *Comput. Chem. Eng.* **2016**, *94*, 370–386. [CrossRef]

23. Ahmad, S. Heat Exchanger Networks: Cost Tradeoffs in Energy and Capital. Ph.D. Dissertation, University of Manchester Institute of Science and Technology (UMIST), Manchester, UK, 1985.

24. Ravagnani, M.; Silva, A.; Arroyo, P.; Constantino, A. Heat exchanger network synthesis and optimisation using genetic algorithm. *Appl. Therm. Eng.* **2005**, *25*, 1003–1017. [CrossRef]

25. Yerramsetty, K.M.; Murty, C. Synthesis of cost-optimal heat exchanger networks using differential evolution. *Comput. Chem. Eng.* **2008**, *32*, 1861–1876. [CrossRef]

26. Huo, Z.; Zhao, L.; Yin, H.; Ye, J. Simultaneous synthesis of structural-constrained heat exchanger networks with and without stream splits. *Can. J. Chem. Eng.* **2013**, *91*, 830–842. [CrossRef]

27. Peng, F.; Cui, G. Efficient simultaneous synthesis for heat exchanger network with simulated annealing algorithm. *Appl. Therm. Eng.* **2015**, *78*, 136–149. [CrossRef]

28. Chen, S.; Cui, G.-M. Uniformity factor of temperature difference in heat exchanger networks. *Appl. Therm. Eng.* **2016**, *102*, 1366–1373. [CrossRef]

29. Castillo, E.; Acevedo, L.; Reverberi, A.P. Cleaner Production of Nitric Acid by Heat Transfer Optimization: A Case Study. *Chem. Biochem. Eng. Q.* **1998**, *12*, 157.

30. Silva, A.P.; Ravagnani, M.A.S.S.; Biscaia, E.C.; Caballero, J.A. Optimal heat exchanger network synthesis using particle swarm optimization. *Optim. Eng.* **2010**, *11*, 459–470. [CrossRef]

31. Pavão, L.V.; Costa, C.B.B.; Ravagnani, M.A.D.S.S.; Jiménez, L. Large-scale heat exchanger networks synthesis using simulated annealing and the novel rocket fireworks optimization. *AIChE J.* **2016**, *63*, 1582–1601. [CrossRef]

32. Aguitoni, M.C.; Pavão, L.V.; Siqueira, P.H.; Jiménez, L.; Ravagnani, M.A.D.S.S. Heat exchanger network synthesis using genetic algorithm and differential evolution. *Comput. Chem. Eng.* **2018**, *117*, 82–96. [CrossRef]

33. Björk, K.M.; Pettersson, F. Optimization of Large-scale Heat Exchanger Network Synthesis Problems. *Model. Simul.* **2003**, *24*, 313–318.

34. Björk, K.-M.; Nordman, R. Solving large-scale retrofit heat exchanger network synthesis problems with mathematical optimization methods. *Chem. Eng. Process. Process. Intensif.* **2005**, *44*, 869–876. [CrossRef]

35. Hu, X.; Cui, G.; Xu, H.; He, Q. Influent of optimization order of heat exchanger on the global optimization result of heat exchanger networks. *Chem. Ind. Eng. Prog.* **2012**, *31*, 987–991.

36. Chen, P.; Luo, N. Differential evolution algorithm with competition mechanism for simultaneous synthesis of heat exchanger network without split streams. *J. East China Univ. Sci. Technol.* **2019**, *45*, 970–979.

37. Chen, S.; Luo, N. Sample average approximation based double-layer improved particle swarm optimization for heat exchanger network synthesis without split streams. *J. Chem. Eng. Chin. Univ.* **2018**, *32*, 620–627.

38. Pavão, L.V.; Costa, C.B.B.; Ravagnani, M. Heat Exchanger Network Synthesis without stream splits using parallelized and simplified simulated Annealing and Particle Swarm Optimization. *Chem. Eng. Sci.* **2017**, *158*, 96–107. [CrossRef]